Article

Wear Reduction on the Roller–Shoe Mechanism at High Operation Loads

Constantin Răzvan Iordache [1], Carmen Bujoreanu [1,*], Stelian Alaci [2], Florina-Carmen Ciornei [2,*] and Ionut-Cristian Romanu [2]

[1] Mechanical Engineering, Mechatronics and Robotics Department, "Gheorghe Asachi" Technical University, 700050 Iasi, Romania; constantin-razvan.iordache@academic.tuiasi.ro

[2] Mechanics and Technologies Department, Stefan cel Mare University of Suceava, 720229 Suceava, Romania; stelian.alaci@usm.ro (S.A.); ionutromanucristian@usm.ro (I.-C.R.)

* Correspondence: carmen.bujoreanu@academic.tuiasi.ro (C.B.); florina.ciornei@usm.ro (F.-C.C.)

Abstract: The roller–shoe mechanism is a classic mechanical assembly with an essential role in motion transmission. Common rail high-pressure pumps are an example of a complex assembly that uses such a mechanism to transform the rotation motion into a translation one. The rolling element of the mechanism is represented by a cylindrical roller. Although it can carry heavy loads due to its design, a proper surface profile could significantly increase the life of the entire mechanism. A better solution can be achieved using a logarithmic profile. The shoe is the second base element of the mechanism. It is a part with an inner cylindrical surface and it is separated from the roller by a thin lubricant film. Considering this, increasing the hardness of the roller–shoe contact surface can be obtained using a suitable coating. The positive results of this coating are highlighted using endurance tests to which high-pressure pumps are subjected. Therefore, the roller profile and the shoe coating represent two directions for improving the contact between the mechanism transmission elements, in terms of wear reduction. The purpose of this paper is to identify a suitable roller profile and to highlight its impact on the shoe coating.

Keywords: roller–shoe; high-pressure pump; coating; logarithmic profile; FEM analyses; endurance tests

1. Introduction

The high-pressure pump is the centerpiece of the common rail system for diesel cars and is its most important component. It is driven by the engine crankshaft via a toothed belt connected to gear wheels or a chain at a 1:1 gear ratio, and its main role is to compress the fuel to pressures in excess of 2000 bar. Fuel under pressure is delivered from the pump to the engine combustion chamber through the high-pressure pipes, the high-pressure rail, and the injectors [1].

Over time, there have been various constructive solutions for high-pressure pumps, depending on the motion transmission mechanism. There are cam–follower and roller–shoe transmission mechanisms. The roller–shoe mechanism is notable for its effective performance and economical production costs. Therefore, it has become a favored solution that captures the attention of all automotive manufacturers. The roller, identified as a rolling component within this mechanism [2], has a cylindrical shape, with its profile being an important factor in wear reduction. This is crucial because, upon contact with the work surface, maximum pressure is applied to the ends. Manufactured from a wear-resistant material characterized by high hardness, it exhibits excellent resistance in high temperature scenarios dictated by the operational requirements. The subsequent component in the mechanism, namely the shoe, is composed of a robust material that is perfectly compatible with the roller. Designed to withstand shocks and crushing, the shoe also facilitates the optimal adhesion of the lubricating fluid. Its durability and hardness are enhanced through

the application of a Diamond-Like Carbon (DLC) coating [3]. The camshaft serves a pivotal role in transmitting the movement of the roller–shoe mechanism, maintaining constant contact with the roller. This is a critical component due to its continuous interaction with the roller. Given the stringent performance requirements of the high-pressure pump, its components experience increasingly heavy loads, resulting in severe wear. Over time, various strategies have been developed to improve their efficiency, including modifications in size, materials, or surface characteristics [2]. These modifications aimed to mitigate wear on the high-pressure pump.

The roller–shoe motion transmission mechanism is the central subassembly of the common rail high-pressure pump. Its wear is important because it can lead to the total failure of the pump. For this reason, it is necessary to find solutions to increase the lifetime of its components. By examining the operation of the motion transmission mechanism, along with its construction and overloading, various approaches are explored. These include the study of lubrication, coatings, and surface profiles.

An essential factor influencing the wear of the mechanism is the quality of the lubrication. This is important to minimize energy loss, heat generation, the wear of the mechanical components, as well as smooth machine operation. Production and productivity are highly dependent on the lubrication system [4]. The lubrication process in high-pressure pumps involves the use of fuel, specifically diesel in our context. The efficacy of diesel fuel in preventing or mitigating wear on the contacting components is diminished, primarily due to its low viscosity. Contact surfaces within high-pressure pumps are safeguarded against wear through the transition from hydrodynamic lubrication to boundary lubrication regimes. In the hydrodynamic lubrication regime, a fluid film acts as a barrier, preventing direct contact between the surfaces [5]. It represents an ideal case of roller–shoe assembly operation. In this way, the lubricant thickness does not allow direct contact between the two components, which leads to the long service life of the components. If a high-pressure pump could constantly run in this regime, a coating for the components would not be necessary. However, this case is not often encountered in roller–shoe contact. The boundary lubrication regime is often reached when there are high loads on the roller, or even more so, when it is operating at low speeds [6]. In this way, the two components come into direct contact. Initially the contact is between the outer diameter surface of the roller and the Diamond-Like Carbon (DLC) layer that is applied to the shoe. Due to high loads, the contact surface extends to the intermediate layer (or the connecting layer) and finally reaches the base material. These aggravating cases lead to scuffing.

Due to the specific working conditions of high-pressure pumps (low speed, high pressure or high fluid temperature), which cannot be modified, it is necessary to investigate new solutions for wear reduction. As a result, our paper is focused on roller profile improvement and the impact of this change on the coating layer. For this purpose, we identified the most used profiles in the literature and assigned them to a cylindrical roller, adapting them according to the requirements of use. To be able to analyze the effect of their use, we performed a simulation in a finite element analysis program and validated the best result through experimental endurance tests. Finally, we performed an analysis of the shoe coating and the material.

2. Considerations Regarding the Improvement of the Roller–Shoe Contact

2.1. Coating Analysis

Interest in the use of coatings has been observed in most assemblies with components that are in contact. They are mainly used to improve wear resistance, friction coefficient, electrical properties, corrosion protection, and last but not least to increase the hardness of the components [7]. The mechanical coating properties have an important role in the reliability of the components to which they are applied. If they are inadequate, this can lead to damage to the components and also to the loss of their role in the assemblies of which they are a part [8]. Thorough adhesion testing is essential to ensure the long-term performance of coated components. There are many methods commonly used to test

the adhesion of coatings to the underlying steel base of the components. Among them, we can list the following: indentation test, scratch test, peel test, blister test, and tensile test [9]. Under oil-lubricated conditions, DLC-coated elements showed a superior wear performance (hardness above 60 HRC) and a reduced friction coefficient compared to other types of coatings [10]. This type of coating has a chemical structure that is often used in the automotive industry (for valves, components of injection systems, transmissions, etc.). It is a type of carbon material that exhibits some of the properties of diamond (hardness or wear resistance). At the base is an amorphous hydrogenated carbon (a:C:H). The process by which this coating is achieved is PACVD (Plasma-Assisted Chemical Vapor Deposition). This is a thin film deposition process (according to our measurements, the DLC layer is about 2 microns) that involves the use of plasma to catalyze the chemical reactions required to deposit the desired material onto the surface of a component. To improve the adhesion of the coating to the underlying steel base in the shoe component, an intermediary layer is integrated.

The coating layer adhesion is performed with a special test called the Rockwell-C adhesion test [11]. This test method is simple and is performed by pressing a diamond cone on the coated surface with a certain force (approx. 1500 N) [12]. The trace left on the coating layer is evaluated under a microscope (Figure 1) and compared with a visual standard [13,14].
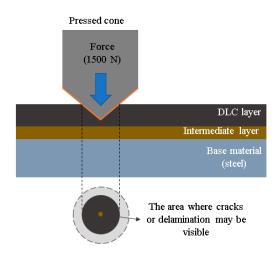

Figure 1. DLC adhesion test—testing method.

In a roller–shoe transmission mechanism, the coating is an important factor for reducing wear, which is already achieved by covering the shoe. It is a difficult task for manufacturers to change it, due to the complexity of the process and the high costs. Thus, another way of reducing wear that we can focus on is modifying the roller profile and analyzing the coverage after this change.

2.2. Roller Profile

By analyzing the motion transmission mechanisms with a cylindrical roller, we could see that there is concern about the contact between the rolling/sliding element and the fixed element. The contact problem of such a mechanism is similar to that of bearings. In the literature, there are various studies that analyze the contact between the roller and the support surface and its influence on wear [15–17]. The roller profile has a particular importance on components in direct contact because under various loads applied to the shoe, it should minimize the stress and increase the life of the two components. In the literature, it was observed that it is difficult to find a universal algorithm for an optimum profile of a particular roller. Most of the time, for economic reasons, it is necessary to create a simple profile [18]. In any cylindrical roller assembly, the load is transmitted through concentrated contacts characterized by small surfaces and very high pressures [19].

Cylindrical rollers are designed to carry substantial radial loads; however, their role in the lifetime of an assembly can be compromised by misalignment and end effects [20]. There are various types of profiles, of which the most common and most analyzed are straight, elliptical, and logarithmic (Figure 2) [21,22].
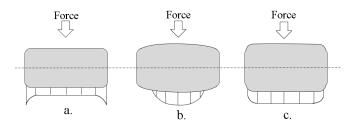

Figure 2. Types of roller profiles: (**a**) straight; (**b**) elliptical; (**c**) logarithmic.

In general, when there is a motion transmission assembly that includes a roller of finite length, the pressure distribution along the roller tends to be more concentrated at the ends than at the center [23]. The occurrence of pressure concentration, known as edge loading or edge effect, intensifies undesirable conditions. This situation is particularly intensified when the roller experiences misalignment due to factors such as mounting errors, thermal errors, or shoe distortion in our case. To attenuate this issue, cylindrical rollers should undergo axial profiling, ensuring a more uniform stress distribution and preventing the occurrence of edge peaks. Following analytical calculations, a logarithmically expressed curve was expressed between two cylinders aligned in contact. Thus, a uniform pressure distribution and a rectangular contact area are obtained [18]. The shape of the measured roller profile from a high-pressure pump is depicted in Figure 3. The highlighted area indicates premature wear [24].
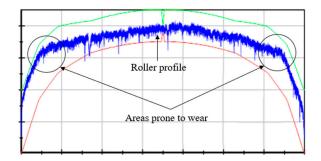

Figure 3. Profile of a high-pressure pump roller.

As previously noted, the three profiles (straight, elliptical, and logarithmic) can be adapted for application to a cylindrical roller within the transmission mechanism of a high-pressure pump. To facilitate this adaptation, a theoretical analysis is imperative for obtaining the profile generators through mathematical means.

3. Roller Profile Theoretical Improvement

The durability of cylindrical roller assemblies is closely connected to the loads that occur within these mechanisms. In both bearings and roller–shoe assemblies, due to the higher pressures on the edges of the roller rather than the central area, even at moderate loads, they can have premature component wear. In order to avoid plastic deformations, it is necessary to use a modified roller profile that is adapted according to the demands, which leads to a uniform pressure distribution [25].

A straight profile is the simplest solution to achieve the contact surface of the roller with the shoe or the shaft. The advantages of this solution are represented by the reduced costs for part design and the manufacturing process. Over time, various tests have been carried out that highlight the fact that a roller with such a profile has high loads on the

ends [26]. Also, the performance requirements of high-pressure pumps (Delphi, Iasi, Romania) have increased, necessitating new, more efficient solutions. The performance of a high-pressure pump is closely related to the fuel pressure it can deliver. As this pressure increases, the wear on its components will increase due to overloading. Thus, the operating parameters will be changed and, implicitly, technical improvement solutions will need to be sought to reduce wear. Using two basic mathematical functions, we built the following graphic representation (Figure 4).

Figure 4. Straight roller profile representation in graphic coordinates.

High-stress distributions on the straight profile roller ends can be reduced by modifying the profile [16]. Thus, a new profile solution for the roller–shoe assembly is an elliptical profile. This can be obtained based on mathematical functions (Equations (1) and (2)) with the help of which we can create an elliptically-shaped profile generator. The role of the constant k is to globally determine the shape of the elliptic curve. A graphical representation of the profile based on Equations (1) and (2) is shown in Figure 5.

$$f_1(x), f_2(x) : [0, a] \to R$$

$$f_1(x) = \frac{b}{2} + \sqrt{\frac{b^2}{4} + \frac{ax - x^2}{k^2}} \tag{1}$$

$$f_2(x) = \frac{b}{2} - \sqrt{\frac{b^2}{4} + \frac{ax - x^2}{k^2}} \tag{2}$$
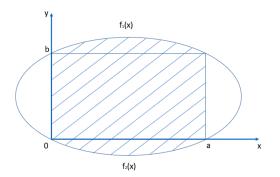

Figure 5. Representation of an elliptical roller profile.

Another roller profile, as a solution for improved contact and reducing wear, is a logarithmic one. As we can see in Figure 6, the logarithmic profile of a cylindrical roller refers to its cross-sectional shape, which is obtained by applying Equations (3) and (4). In this instance, the roller's diameter undergoes a specific variation along its axis, ensuring that the cross-section of the roller adheres to a logarithmic curve.

$$f_1(x), \ f_2(x) : [0, \ a] \to R$$

$$f_1(x) = b + \alpha ln \left[1 + \beta \left(\alpha x - x^2 \right) \right] \tag{3}$$

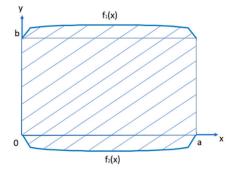$$f_2(x) = -\alpha ln\left[1 + \beta\left(\alpha x - x^2\right)\right] \tag{4}$$

Figure 6. Representation of a logarithmic roller profile.

Equations (3) and (4) are developed with the help of elementary functions composed according to the requirements imposed (generation of a logarithmic profile curve). The curvature constants α and β determine globally (starting from central area) and locally (at the roller ends) the shape of the logarithmic curve. These can be arbitrarily chosen so that the resulting profile can minimize contact pressure distributions on overloaded areas.

To observe the impact of each profile in minimizing stress, we performed a finite element analysis. Thus, we can study the evolution of contact pressures, equivalent stress, specific deformations, and contact forces under real operating conditions.

4. Simulation of the Transmission Mechanism Operation

A numerical simulation is carried out on the entire transmission mechanism, composed of shoe, roller, and shaft cam. The shaft cam is vertically positioned, thus the piston is at the top dead center, compressing the fluid in the compression chamber.

4.1. Component Design in Catia

The program used for the design of the element's parts is Catia (Catia V5 r19) (Figure 7).
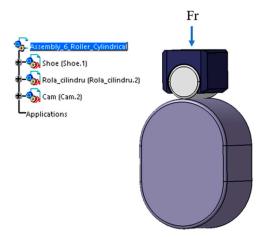

Figure 7. Transmission mechanism elements made in Catia V5 for simulation.

Designing the straight profile roller is a simple process, which does not imply a special mathematical function in the design program. Thus, using the basic commands and taking into account the dimensional characteristics, we were able to obtain a 3D variant for the straight profile roller (Figure 8).
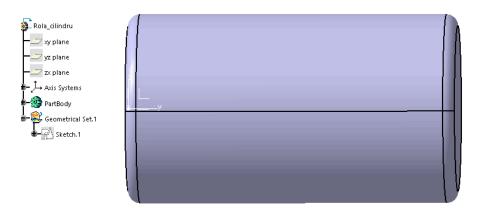
Figure 8. Roller with straight profile (3D view).

Using the Equations (1) (Figure 9) and (2) and the values from Table 1 is obtained the elliptical profile (Figure 10) of the cylindrical roller in the Catia V5 program. The values from the table are the measured dimensions from a real roller–shoe transmission.

Figure 9. Equation (1) introduced in the Catia design program.

Table 1. Dimensions and constants values for generating the elliptical profile.

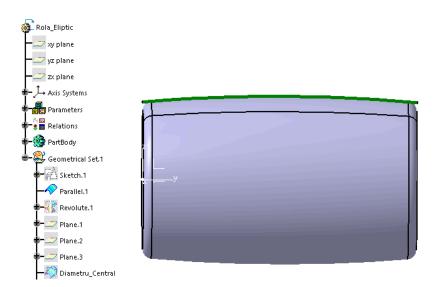| Dimension/Constant	Value	Comments
Roller length	21 mm	Measured parameter
Roller diameter	12,029 mm	Measured parameter
k	3	Constant with arbitrarily chosen value, k > 0

Figure 10. Elliptical profile generator.

The logarithmic profile is another improved version compared to the previous ones. Referring to the complexity of the roller manufacturing process, creating a logarithmic profile is a high-precision operation that is susceptible to processing deviations.

By entering Equation (3) and the values from Table 2 in the Catia program (Figure 11) we obtain the logarithmic profile generator (Figure 12).

Table 2. Values for dimensions and constants needed to calculate the logarithmic profile.

Dimension/Constant	Value	Comments
Roller length	21 mm	Measured parameter
Roller diameter	12,029 mm	Measured parameter
α	0.003	Constant with arbitrarily chosen value, k > 0
β	0.056	Constant with arbitrarily chosen value, k > 0

Figure 11. Introduction of calculation relationship in Catia.

Figure 12. The logarithmic profile generator for the cylindrical roller.

4.2. FEM Analysis Technical Details

The purpose of this simulation is to observe the evolution of the pressure distribution at the roller–cam contact when the roller has various profile shapes (straight, elliptical, and logarithmic profile). The simulation is statically performed using the ANSYS program. To obtain a realistic result, we take into account the forces acting in the vertical direction (Fr) and the friction coefficients from Table 3. These friction coefficients were obtained using the Castro relation [27] and also considering the constructive and usual running conditions of the mechanism [28]. The roller–shoe and roller–cam friction forces are calculated directly using the ANSYS program, at the required pressures, and it is only necessary to enter the friction coefficients according to the type of materials.

Table 3. Friction coefficients used on the ANSYS simulation.

Components in Contact	Coefficient Value
Roller–shoe friction coefficient	0.059
Roller–cam friction coefficient	0.076

The sum of the forces acting in the vertical direction in the four phases of operation (phase 1—cranking, phase 2—idle, phase 3—maximum torque, phase 4—maximum power) of the high-pressure pump will be taken into account (Table 4).

Table 4. Roller–shoe mechanism radial forces.

Operating Phase	Total Force Fr [N]
Phase 1	878.42
Phase 2	1574.78
Phase 3	6051.38
Phase 4	7444.1

In order to achieve an optimal balance of convergence and validity of the results, with the aim of obtaining applicable results in a similar manner to all the simulations in this study, we finally chose hexahedral elements (with six faces). These elements are known for providing high precision results.

Following the discretization tests, with different values of the mesh, we found a fine configuration to be optimal, as a coarse discretization mesh provided imprecise distributions of pressures, equivalent stresses, and specific strains. A fine discretization mesh also offers the advantage of eliminating the pressure and stress concentration values, with optimal element size values leading to the convergence of finite element analysis results, whilst also involving higher processing time.

For the simulations, we considered Augmented Lagrange frictional contacts (using the friction coefficients established in Table 3). Alternative contact formulations such as Normal Lagrange, MPC (Multiple Point Constraints), or Pure Penalty would have provided similar but inconsistent results across the duplication of simulations, discretization grid, and solver parameters (Analysis Settings).

We opted to exclusively examine the interaction between the roller and the cam, as the inclusion of the shoe amplifies the non-linearity of the assembly. This causes convergence issues. Consequently, our simulations concentrated only on the components that best illustrate the impact of the roller profile. In order to avoid cases of non-convergence of the analyses, we opted for a simple application of the contour conditions. This consists in embedding on the side faces of the cam and pressing the roller with the force values (Table 4). Additionally, using a translational joint, we ensured that the roller has a displacement in the vertical direction, thus restricting the model even better and ensuring full success when running the simulations (Figure 13).
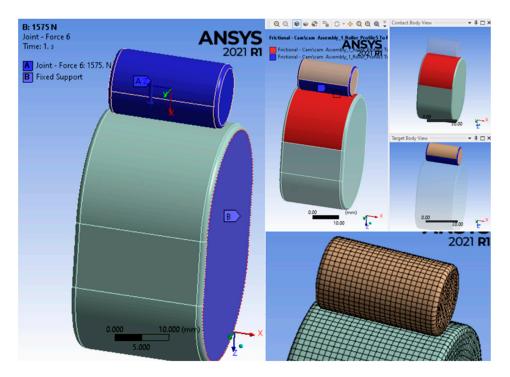

Figure 13. Roller–cam contact in ANSYS program.

4.3. ANSYS Simulation Results

We studied, in simulation, the three roller profiles.

The straight roller profile develops contact forces and pressures, equivalent stress, and moderate specific strains, but with peaks at the ends of the roller contact area. This is visible in both the surface and the section distributions (Figure 14).

The simulation results of the contact between the cam and the roller with an elliptical profile show increased values of contact pressures, stresses, and strains (Figure 15). The load concentrations on the central area, together with the high values of the analyzed parameters, lead to high wear for the roller and cam.
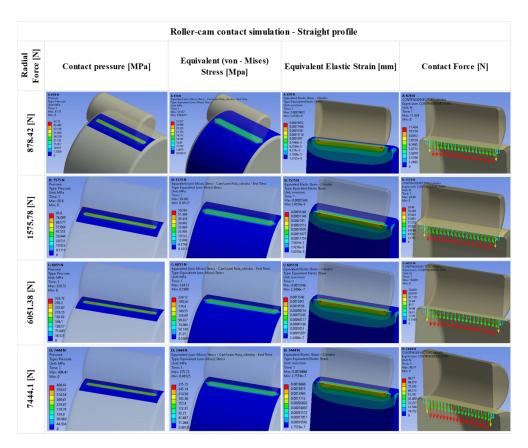
Figure 14. Simulation results of contact between cam and straight profile roller.
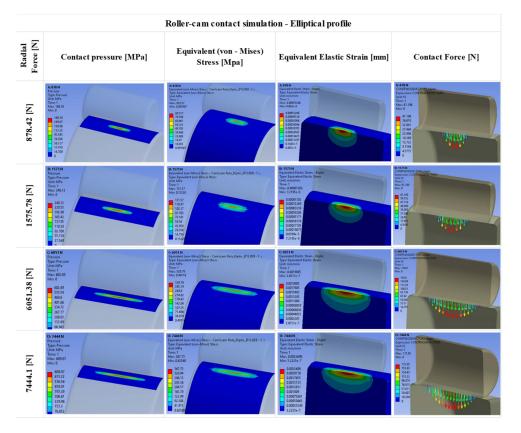

Figure 15. The simulation results of the contact between the cam and the roller with an elliptical profile.

The simulation of the roller–cam contact with a logarithmic profile reveals a noticeable improvement when high forces are applied to the mechanism. A better dispersion of the contact pressures and the equivalent stresses are visible. Also, the contact force vectors along the roller show a stress-free distribution at the ends (Figure 16), which are shown by the ANSYS program for each individual node, the legend presenting the value of the maximum contact force in that area.
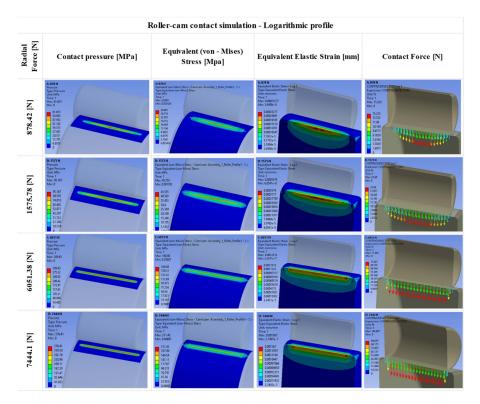

Figure 16. Simulation results of contact between cam and roller with logarithmic profile.

4.4. Simulation Comparative Analysis

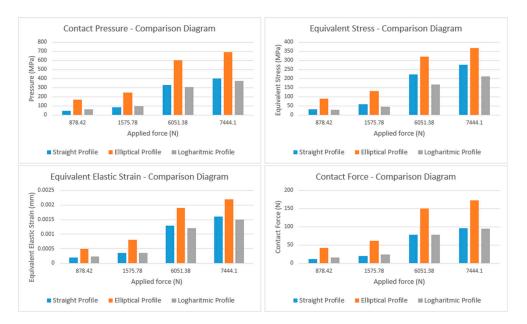Figure 17 provides an overview of the simulation results.

Figure 17. Simulation results overview.

4.4.1. Quantitative Comparisons between Straight Profile Roller and Logarithmic Profile Roller

- The simulation outcomes at a force of 878.42 N reveal an approximately 22% variance in the maximum contact pressure between the straight profile (47.75 MPa) and the logarithmic profile (61.66 MPa), with the latter exhibiting a disadvantageous result. This pattern persists in terms of specific strains and contact forces, showing differences of approximately 15% and 25%, respectively. It is important to mention that this force corresponds to a short operating phase of the vehicle, with little impact on the wear of the motion transmission components.
- When applying the same force (878.42 N), the equivalent stress shows a percentage difference of 9% in favor of the roller with the logarithmic profile (32.56 MPa compared to 29.6 MPa).
- Comparatively analyzing the results when applying the other forces, an obvious improvement is visible for all parameters when we use a logarithmic profile.

4.4.2. Quantitative Comparisons between the Roller with an Elliptical Profile and the Roller with a Logarithmic Profile

- Compared to the maximum contact pressure of 168.38 MPa provided by the straight profile at a force of 878.42 N, the logarithmic profile develops a maximum of 61.66 MPa, showing a decrease of about 63%. This trend is maintained for all parameters, with the percentage difference remaining close to 60%.
- The same favorable percentage difference is maintained in the case of the other applied forces.

5. Experimental Validation

The high-pressure pumps wear can be highlighted based on the performance of experimental tests. The evaluation must be carried out by simulating real operating conditions, which is why the testing process becomes a complex and important stage. The roller–shoe mechanism operates at high forces for most of its working time. After the simulation at high forces, the logarithmic profile shows lower values of the contact parameters (contact pressure, equivalent stress, equivalent elastic strain, and contact force) compared to the straight one. All these parameters are involved in the production of wear and friction [29]. Considering the favorable results of using the logarithmic profile in the simulation and the limited financial resources, we chose to perform a physical test on a single pump, whose transmission mechanism contains such a roller profile. Thus, from a batch of components from the manufacturer, we chose a roller with an identical profile to the one in the simulation and mounted it on a high-pressure pump. We then performed an endurance test on the resulting assembly.

5.1. Testing Methodology

High-pressure pump tests are carried out on special test machines (Bosch EPS 815, Istanbul, Turkey) (Figure 18). They are equipped with measurement sensors for pressures, flows, temperatures or speeds, parameters that can be checked in real time. The test algorithm is adapted so that we can obtain a wide range of values for these parameters of interest. Based on this test, a detailed analysis of the contact surface of the roller–shoe is pursued. For this reason, the chosen test is a static one, through which we can maintain constant values of the above-mentioned parameters for a period of approximately 20 h. The aggravating test conditions are achieved by reducing the fluid film between roller and shoe. Thus, we imposed a reduced speed (approx. 400 rpm) for the pump shaft, a high pressure for the fluid exiting the pump (approx. 2000 bar) and, at the same time, a high temperature for this fluid (approx. 120 degrees). The testing fluid has diesel-like properties.
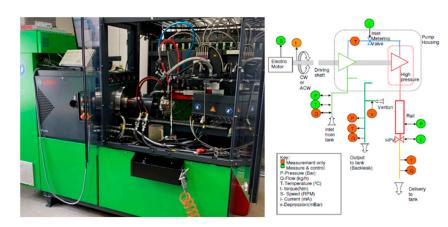
Figure 18. Special bench for testing high-pressure pumps.

5.2. Testing Data Analysis

The analysis of the data obtained from the test bench is carried out by carefully monitoring the evolution of the important parameters of the high-pressure pump. The monitored parameters are shaft speed, pressure, and temperature. The experimental data are taken from the test bench, after which graphs are made. They indicate the evolution of the parameters throughout the test (Figure 19).
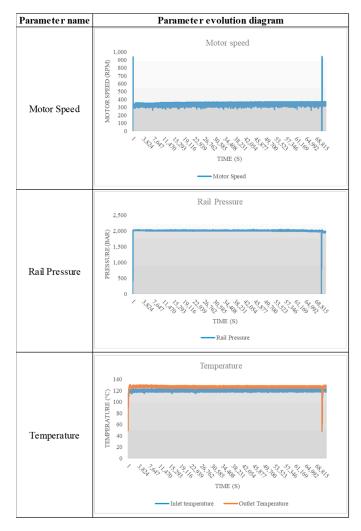
Parameter name	Parameter evolution diagram
Motor Speed	
Rail Pressure	
Temperature	

Figure 19. Test parameters evolution.

The results do not indicate deviations from the values initially imposed on the parameters. The speed and pressure keep setpoints constant during the test. The temperature on the pump return has a slight increase due to the friction of the pump's internal components. Two peaks are visible on the graphs (at the beginning and at the end). The first is due to the initialization period of the pump (in which the parameter values were imposed). The one at the end is caused by the maintenance period (oil and filter change) of the test bench.

5.3. Drive Train Component Visual Analysis

The high-pressure pump (Delphi, Iasi, Romania) is disassembled in order to observe the condition of the transmission mechanism elements (Figure 20). We perform this visual inspection to confirm the results of the test bench data analysis.

Figure 20. Transmission mechanism visual condition.

There are no friction marks on the ends of the roller, the surface condition being the same along its entire length. The inner surface of the shoe is similar to the surface of a new component. No areas of coating removal or circular contact streaks are observed. This indicates a very low level of wear due to uniform contact with the roller. The shaft cam shows no signs of wear or overheating. The contact area of the cam with the roller is easily visible, without overheated areas on the edges. Considering the experimental test and also the simulation results, the logarithmic roller profile is beneficial for the wear behavior of the transmission mechanism. Finite element analysis is a basic tool for the design of any product, and the comparison between the straight and the logarithmic profiles showed the superiority of the latter in terms of wear reduction. Therefore, experimental testing is performed only on the assembly that shows the best results, without the need to waste resources.
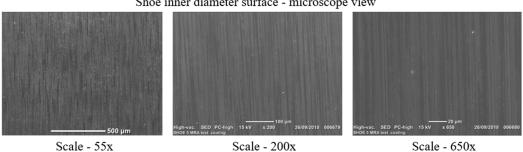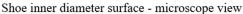
6. Shoe Coating and Material Analysis

Using the tested logarithmic profile, we can study its impact on the shoe surface, more specifically on the coating layer. This analysis involves measuring the hardness and coating layer adhesion in the areas where there is greater friction between the components. We performed hardness measurements and adhesion tests according to the VDI 3198 standard [13].
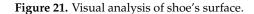
6.1. Hardness Measurement

Hardness is measured using the Vickers method [30]. This is used more often for small parts. To check material hardness, it is necessary to cut the piece on the most initial overloaded area (central area).

This allows for measuring the hardness of the material on the contact area. Before doing this, we visually checked the surface of the shoe's inner diameter under a microscope (SEM FEI Quanta 200 3D microscope, Brno, Czech Republic) (Figure 21). It had no defects.

Shoe inner diameter surface - microscope view

Scale - 55x   Scale - 200x   Scale - 650x

Figure 21. Visual analysis of shoe's surface.

To obtain the hardness at the six points, using the Vickers method, the time the durometer tip is held on the surface of the shoe is 10–15 s. We used a period of about 12 s for all six measurements.

Figure 22 exposes the six measurement positions. The results obtained after measuring the hardness have a constant trend and are around the value of 700 HV (Figure 23). Measurements were made both in depth and towards the edge area to observe if the changes in hardness (its decrease) were caused by the increase in temperature due to the intense friction. The fact that all these values are high and constant indicates the preservation of the original properties of the material and the reduced friction obtained as a result of the profile improvement.
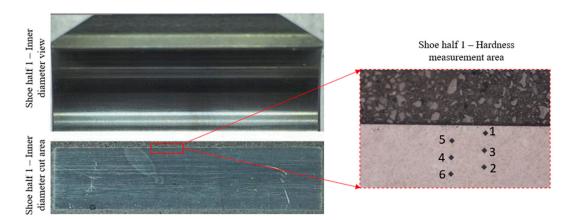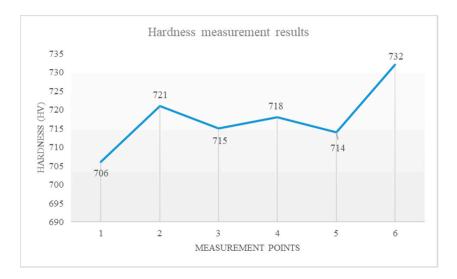

Figure 22. Hardness measurement area.

Figure 23. Hardness measurement results.

6.2. Coating Adhesion Test

As mentioned in the introductory part, the adhesion test is an important solution for evaluating the DLC layer. Thus, following the directions described, we decided to evaluate the Diamond-Like Carbon layer after testing the high-pressure pump. To assess the defect, we used the visual standard in Figure 24. An acceptable result predicts an increased life of the shoe.
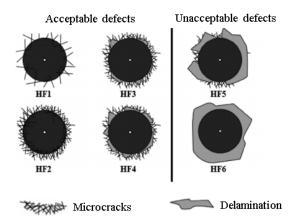

Figure 24. DLC adhesion test visual standard.

Considering the mark left on the part surface (Figure 25) and comparing it with the visual standard, we considered that the adhesion test shows a positive result. It falls between the values of standards HF2 and HF3. Although there are not many cracks, a slight delamination can be observed in a few areas, which is why we chose this approximation. Considering the operating parameters of the pump and the fact that this delamination does not cover large surfaces, this was considered a good result.
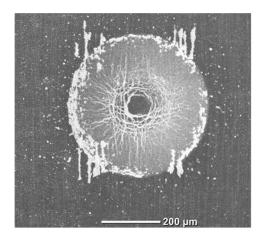

Figure 25. Trace left on the shoe surface.

7. Conclusions

The components inside a pump are lubricated with diesel fuel. Its viscosity is low compared to other lubricants but it is impossible to modify the lubricant, considering its use in the common rail system. The lubrication of a roller–shoe assembly can migrate in various regimes, over different periods of time, depending on the operating mode of the vehicle. Considering that diesel fuel is the only fluid that can circulate in a pump, we focus on the roller profile and its influence on the shoe contact surface. Improving the roller profile can be easily implemented in the production process. Thus, initially we theoretically analyzed different types of profiles that are already used on cylindrical rollers. In order to observe their impact on the roller of the transmission mechanism, we performed a simulation of its

operation in the ANSYS program. The simulation results show an obvious improvement of the pressure distribution when we use a logarithmic profile calculated for the cylindrical rollers compared to the straight and elliptical profiles. This result was validated by an experimental test, which indicated a guaranteed applicability. The coating analysis is an additional analysis carried out to observe the roller profile improvement impact on this. By analyzing the clean surface of the shoe, free of defects, we can consider that the DLC is an anti-friction solution that can still be used on such parts. This is also confirmed by the sufficient adhesion, the result of which falls within the acceptable area. These analyses were performed on the actual mechanism and are not found in the literature. The study is based on the interaction between theory and automotive exploitation conditions, where high-pressure pumps are used. The developed solution was designed so that it can be applied in the industrial environment, respecting the trend of improving performance indicators (time and cost).

Author Contributions: Conceptualization, C.R.I. and C.B.; methodology, C.R.I.; software, S.A. and I.-C.R.; validation, C.R.I. and F.-C.C.; investigation, I.-C.R.; writing—original draft preparation, C.B. and C.R.I.; writing—review and editing, F.-C.C. and S.A.; supervision, C.B.; All authors have read and agreed to the published version of the manuscript.

Institutional Review Board Statement: Not applicable.

Informed Consent Statement: Not applicable.

Data Availability Statement: Data are contained within the article.

Conflicts of Interest: The authors declare no conflicts of interest.

References

1. Yue, G.; Qiu, T.; Dai, H.; Lei, Y.; Zhao, N. Rail pressure control strategy based on pumping characteristics for the common rail fuel system. *Adv. Mech. Eng.* **2018**, *10*, 1687814018795591. [CrossRef]
2. Jorach, R.W.; Bercher, P.; Meissonnier, G.; Milovanovic, N. Common Rail System from Delphi with Solenoid Valves and Single Plunger Pump. *Auto Tech Rev.* **2012**, *1*, 38–43. [CrossRef]
3. Ghasemi, M.H.; Ghasemi, B.; Semnani, H.R. Wear performance of DLC coating on plasma nitrided Astaloy Mo. *Diam. Relat. Mater.* **2019**, *93*, 8–15. [CrossRef]
4. Vishwakarma, S.K. *Lubrication System*; DIT University: Uttarakhand, India, 2015.
5. Abdelbary, A.; Chang, L. *Principles of Engineering Tribology: Lubrication and Surface Engineering (Book Chapter)*; Elsevier: Amsterdam, The Netherlands, 2023; Volume 7, pp. 295–343.
6. Sadeghi, F. *Elastohydrodynamic Lubrication. Tribology and Dynamics of Engine and Powertrain*; Woodhead Publications: Cambridge, UK, 2010; pp. 171–226.
7. Iost, A.; Bigot, R. Hardness of coatings. *Surf. Coat. Technol.* **1996**, *80*, 117–120. [CrossRef]
8. Malzbender, J.; den Toonder, J.M.; Balkenende, A.R.; de With, G. Measuring mechanical properties of coatings: A methodology applied to nano-particle-filled sol–gel coatings on glass. *Mater. Sci. Eng. R Rep.* **2002**, *36*, 47–103. [CrossRef]
9. Chen, Z.; Zhou, K.; Lu, X.; Lam, Y.C. A review on the mechanical methods for evaluating coating adhesion. *Acta Mech.* **2013**, *225*, 431–452. [CrossRef]
10. Cho, D.-H.; Lee, Z.Y. Evaluation of Ring Surfaces with Several Coatings for Friction. *Wear Scuffing Life Trans. Nonferrous Met. Soc. China* **2009**, *19*, 992–996. [CrossRef]
11. Broitman, E.; Hultman, L. Adhesion improvement of carbon-based coatings through a high ionization deposition technique. *J. Phys.* **2012**, *370*, 012009. [CrossRef]
12. Laszlo, N. Investigation of Adhesion Behaviour of Different Underlayered DLC Coated Cold Forming Tool Steel. *U Porto J. Eng.* **2021**, *7*, 60–68. [CrossRef]
13. Vidakis, N.; Antoniadis, A.; Bilalis, N. The VDI 3198 indentation test evaluation of a reliable qualitative control for layered compounds. *J. Mater. Process. Technol.* **2003**, *143–144*, 481–485. [CrossRef]
14. Adhesion Testing Using the Rockwell Method. Available online: https://www.oerlikon.com/balzers/my/en/portfolio/job-coating-services/our-competencies/measuring-techniques-for-quality-assurance-of-oerlikon-balzers-coatings/ (accessed on 8 January 2024).
15. Puneethkumar, M.V.; Sunil, S. Analysis of contact pressure distribution of the straight and crowning profiles of tapered roller bearing. *Int. J. Mech. Eng. Robot. Res.* **2014**, *3*, 483–493.

16. Shao, Y.; Liu, J.; Ye, J. A new method to model a localized surface defect in a cylindrical roller-bearing dynamic simulation. *Proc. Inst. Mech. Eng. Part J. Eng. Tribol.* **2013**, *228*, 140–159. [CrossRef]

17. Hao, S.; Keer, L.M. Rolling Contact Between Rigid Cylinder and Semi-Infinite Elastic Body with Sliding and Adhesion. *J. Tribol.* **2007**, *129*, 481–494. [CrossRef]

18. Tudose, L.; Tudose, C. Roller profiling to increase rolling bearing performances. *IOP Conf. Ser. Mater. Sci. Eng.* **2018**, *393*, 012002. [CrossRef]

19. Crețu, S.S. The effect of primary loading on fatigue life of cylindrical roller bearings. *IOP Conf. Ser. Mater. Sci. Eng.* **2016**, *147*, 012011. [CrossRef]

20. Drobný, P.; Mercier, D.; Koula, V.; Škrobáková, S.I.; Čaplovič, Ľ.; Sahul, M. Evaluation of Adhesion Properties of Hard Coatings by Means of Indentation and Acoustic Emission. *Coatings* **2021**, *11*, 919. [CrossRef]

21. Bamu, B.; Murthy, V.V.R. Contact Analysis of Cylindrical Roller Bearing Using Different Roller Profiles. *Int. J. Res. Mech. Eng. Technol.* **2013**, *3*, 29–33.

22. Wei, Y.; Qin, Y.; Balendra, R.; Jiang, Q. FE analysis of a novel roller form: A deep end-cavity roller for roller-type bearings. *J. Mater. Process. Technol.* **2004**, *145*, 233–241. [CrossRef]

23. Crețu, S.S. *Mecanica Contactului*; Gh. Asachi Publishing House: Iași, Romania, 2002; Volume 1.

24. Iordache, C.R.; Ciornei, F.C.; Bujoreanu, C. Scuffing analysis of roller-shoe mechanism after an aggressive test. *IOP Conf. Ser. Mater. Sci. Eng.* **2019**, *591*, 012020. [CrossRef]

25. Popescu, A.; Popescu, G. Cylindrical Roller Bearings with Optimized Profile Taking into Account the Material Structure and Operating Temperature. *Bull. Polytech. Inst. Iași. Mach. Constr. Sect.* **2022**, *68*, 109–123. [CrossRef]

26. Wu, Z.; Xu, Y.; Deng, S.; Liu, K. Study on logarithmic crowning of cylindrical roller profile considering angular misalignment. *J. Mech. Sci. Technol.* **2020**, *34*, 2111–2120. [CrossRef]

27. Castro, J.; Seabra, J. Global and local analysis of gear scuffing tests using a mixed film lubrication model. *Tribol. Int.* **2008**, *41*, 244–255. [CrossRef]

28. Iordache, R.C.; Petrea, N.D.; Bujoreanu, C. Study of roller-shoe contact during high-pressure injection pump normal operation. *IOP Conf. Ser. Mater. Sci. Eng.* **2022**, *1235*, 012068. [CrossRef]

29. Jackson, R.L.; Ghaednia, H.; Lee, H.; Rostami, A.; Wang, X. Contact Mechanics. In *Tribology for Scientists and Engineers*; Springer: Berlin/Heidelberg, Germany, 2013; pp. 93–140.

30. Moore, P.; Booth, G. *The Welding Engineers Guide to Fracture and Fatigue*; Elsevier: Amsterdam, The Netherlands, 2015; pp. 175–184.